Dynamic Model Refinement for Buoyant Energy Storage Technology

T. Thornbrue* and R. Ghorbani**

Renewable Energy Design Laboratory
Department of Mechanical Engineering
University of Hawai'i at Manoa
Honolulu, HI, USA
*tt6@hawaii.edu, **rezag@hawaii.edu

ABSTRACT

Methods of utility scale electrical energy storage are continuing to be explored to address issues associated with renewable resource intermittency. A novel concept known as Buoyant Energy Storage Technology (BEST) is presented with a refined dynamic model and simulation demonstrating the performance of a prototype scale system.

With a dual mode AC synchronous machine easily adapted for grid interconnection, a torque regulated control scheme drives a large buoyant element to depth to store energy, while generation harvests energy from its ascent.

Results show competitive round trip efficiencies with response times on the order of seconds. Cost are also expected to be low through the use of commercially available off-the-shelf components, adding further promise to the future of BEST.

Keywords: ocean engineering, energy storage

1 INTRODUCTION

As the use of renewable energy grows, methods of large scale energy storage are being considered as solutions to grid destabilization challenges associated with resource intermittency. As introduced in [1] and [2], Buoyant Energy Storage Technology (BEST) is a promising concept with potential to store and discharge electric energy with a high efficiency and low cost. Though many possible configurations for such a system exist, the simplest embodiment, illustrated in Fig. 1, is being considered to evaluate system performance.

The preliminary dynamic model of this design was previously created and estimated an upper bound round trip efficiency of 92.9% [3]. The model contained only primary sources of force including buoyancy, hydrodynamic drag, and electromotive force from a DC motor. Two separate simulations were conducted for storage and discharge modes of operation, and the results combined to calculate efficiency.

A more comprehensive model is introduced that includes an AC synchronous machine and braking mechanism that enable dual mode operation. This allows for a single simulation to be conducted, demonstrating one complete operational cycle. The addition of gearbox and bearing losses also make the model more realistic, allowing for a refined estimate of efficiency to be calculated.

Experimental methods are explained followed by results, conclusions, and future work.

2 METHODS

As described in [3], dynamic modeling and simulation are performed in the MathWorks® Simulink™ computing environment. Within Simulink is a toolbox known as Simscape™, which is a platform for physical modeling. Instead of connecting together blocks that define the equations of a system, Simscape enables modeling and simulation of multi-domain physical systems, such as those with mechanical and electrical components. Additionally, the Simscape toolbox provides blocks for many common components with validated, preset configurations, greatly expediting the modeling process.

For the sake of brevity, this paper omits the system's defining equations introduced in [3].

2.1 Modeling

A submerged spherical buoyant element of 1.25 m radius creates a buoyant force of 78.8 kN. This force acts vertically on a cable which is wound on a 0.2 m diameter spool. A braking mechanism is used to secure the buoyant element during static periods and to aid in changing directions.

The axle of the spool connects to a gearbox with a gear ratio of 40:1 to reduce torque and increase speed. This is coupled to a 500 V, 50 kW, 8 pole interior permanent magnet synchronous machine (IPMSM) that can act as both a motor and generator through the use of a Permanent Magnet Synchronous Motor Drive (PMSMD) provided by Simscape. The PMSMD is chosen to provide control through torque regulation which is limited to 400 Nm for the speeds used in this simulation.

The PMSMD is powered by a 6.5 Ah, 200 V, 21 kW Nickel-Metal-Hydride battery that connects through a voltage regulated DC/DC converter (boost type). This adapts the low voltage of the battery (200 V) to the

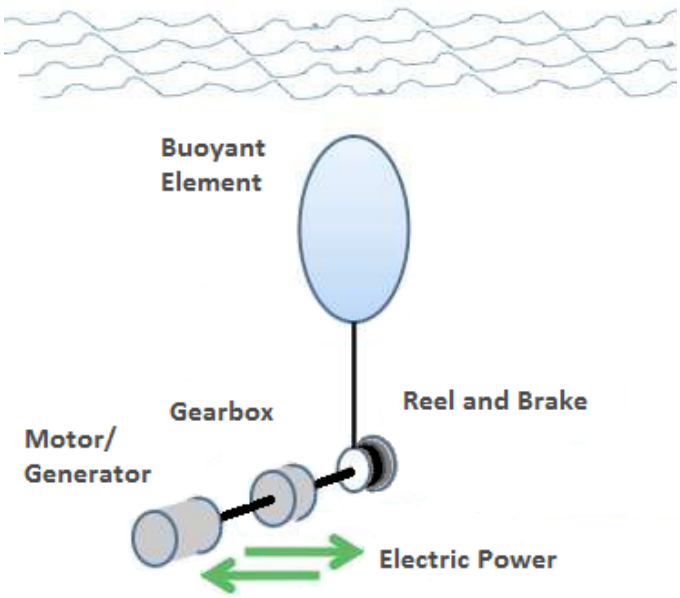

Figure 1: The simplest embodiment of a BEST design. An electric motor drives the buoyant element to depth to store energy. When demand warrants, the element is allowed to rise, this time driving the motor to discharge electricity.

DC bus which feeds the PMSMD at a nearly constant voltage of 500 V. The use of this configuration allows reference monitoring of the state of charge (SOC) of the battery as well as providing a more realistic power source than the previously modeled constant voltage source.

Hydrodynamic drag is modeled as a function of buoyant element velocity squared described in [3], and the addition of damping forces that account for gearbox losses and bearing friction are modeled as functions of angular velocity using

$$\tau_d \;=\; c\,\omega, \tag{1}$$

where τ_d is torgue due to damping, c is the damping coefficient, and ω is angular velocity. On the IPMSM side, a value of 0.1 $\mathrm{Nm}/\frac{\mathrm{rad}}{\mathrm{s}}$ was chosen for c, while 10 $\mathrm{Nm}/\frac{\mathrm{rad}}{\mathrm{s}}$ was chosen on the torque multiplied side of the gearbox.

2.2 Simulation

One goal of constructing a refined model is to allow the use of a single simulation to demonstrate starting and stopping of both storage and discharge modes. The intent is to have the buoyant element start and stop at the same vertical position, then measurements of energy input and output taken to calculate the round-trip efficiency of a complete cycle. Toward this end, a 28 second simulation is constructed using the following timetable of events where storage commences first, followed by discharge. Note that the system starts from rest with the buoyant element at its shallowest position.

Table 1: Timetable of BEST System Control Events

Time(s)	Event
0	Max IPMSM torque to accelerate system
3	Maintain constant descent velocity
10	Zero IPMSM torque to decelerate system
13	Apply brake to secure system
14	Release brake to allow system acceleration
17	Maintain constant ascent velocity
24	Max IPMSM torque to decelerate system
27	Apply brake to secure system
28	End Simulation

3 RESULTS

3.1 Electromechanical Performance

Figures 2 - 4 show the performance of the system in terms of buoyant element position and velocity, as well as motor electrical power, which are explained below.

The maximum torque from the IPMSM is used both to accelerate the buoyant element downward and to decelerate its ascent. At the start of the simulation, this torque is called to accelerate the buoyant element towards a velocity of -14.4×10^{-2} m/s as seen in Fig. 2. This speed keeps hydrodynamic drag low and corresponds to a IPMSM angular velocity of roughly 550 rpm (57.6 $\frac{rad}{s}$).

To maintain these velocities and therefore consume a constant amount of electrical power, a torque of 203.55 Nm is called at 3 seconds and held constant for 7 seconds. Mechanical power (P_{m}) can be calculated using

$$P_{\mathrm{m}} \;=\; \tau \cdot \omega, \tag{2}$$

where τ is torque and ω is angular velocity ($\frac{rad}{s}$). This gives a value of 11.7 kW of mechanical power production during this segment. This value is lower than the measured electrical power between the DC/DC converter and the 3 phase inverter driving the IPMSM which is shown to be 12.0 kW in Fig. 4. Electrical Power (P_{e}) is calculated from measurements of DC current (I) and voltage (V) using

$$P_{\mathrm{e}} \;=\; I\,V. \tag{3}$$

The losses between electrical input and mechanical output can be attributed to internal resistance in the IPMSM and indicate a high efficiency machine.

It is important to note that by changing ω or τ in eqn. (2), mechanical power and therefore electrical power can be manipulated. This can be accomplished by either allowing the system more or less time to reach a desired

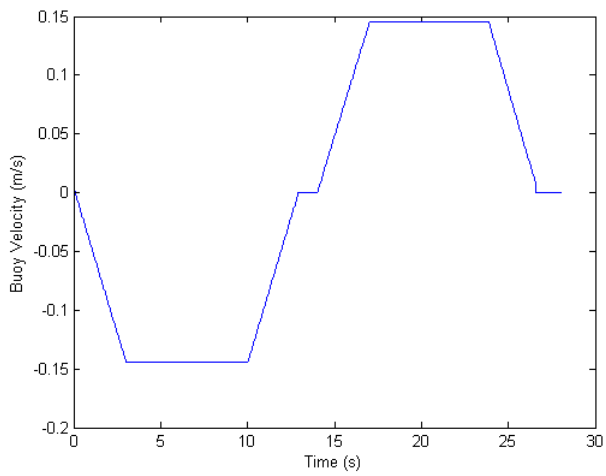

Figure 2: Buoyant element velocity vs. time.

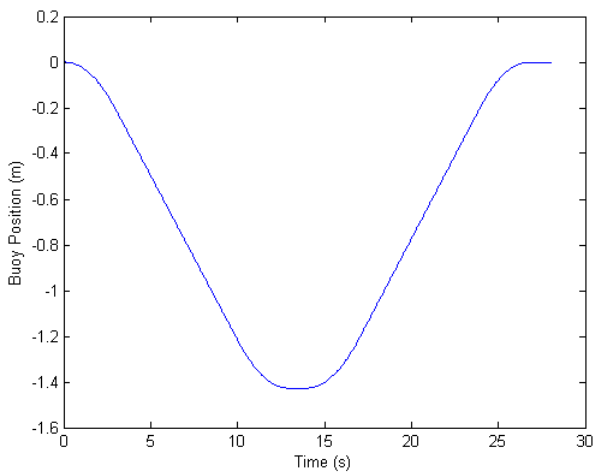

Figure 3: Buoyant element position vs. time.

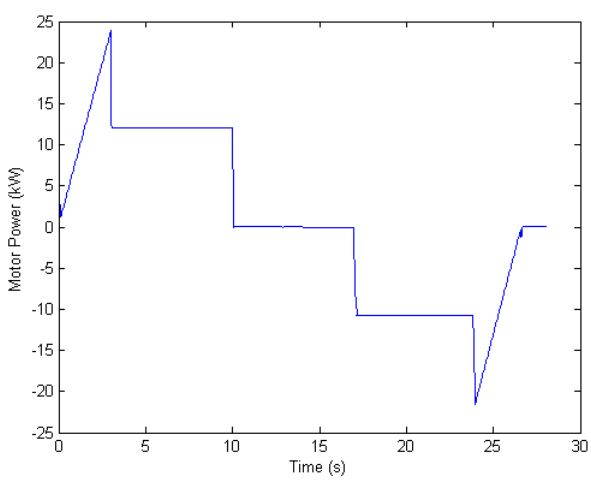

Figure 4: PMSMD power vs. time.

speed (subject to motor limitations), or commanding different torque levels from the motor. The latter forms the basis for a feedback control loop that can smooth the jagged power curve seen in Fig. 4. The time to reach the steady state power level calculated above is only 3 seconds, which is good for grid frequency regulation applications, and also minimizes simulation and therefore computing time.

To decelerate the descent of the buoyant element, IPMSM torque is reduced to zero at 10 seconds, and buoyant force acts to stop the system. Upon reaching nearly zero velocity, the brake is engaged which holds the buoyant element steady for 1 second. It can be seen from Fig. 3 that the buoyant element reached a maximum depth of 1.39 m.

At 14 seconds, the brake is released and the buoyant element is allowed to accelerate upwards to a velocity of 14.5×10^{-2} m/s. At 17 seconds, a torque of 192 Nm is called to maintain velocity and generate constant electrical power. Using eqn. (2), mechanical power consumed during this segment equals 11.1 kW, and using eqn. (3), electrical power generated during this time equals 10.8 kW.

It can be observed that more torque is required to maintain constant velocity for storage mode (buoyant element descent) than for discharge mode (buoyant element ascent). This is attributed to the effects of hydrodynamic drag and rotational friction losses. In storage mode, these losses oppose the action of the IPMSM which is moving the buoyant element downwards; in discharge mode, the losses work in tandem with the IPMSM which is acting to regulate the speed of the buoyant element.

After 7 seconds of stable generation, full IPMSM torque is called to slow the ascent, generating a higher, but rapidly diminishing power level shown in Fig. 4.

After 3 seconds of deceleration, the brake is engaged and the buoyant element becomes steady at its original starting position at 27 seconds shown in Fig. 3. The simulation ends 1 second later.

3.2 System Efficiency

Splitting the power curve into separate storage and discharge curves allows the integration of both, which can then be used to calculate the round-trip system efficiency at the PMSMD (η_m) through

$$\eta_m = \frac{\int_{\text{mid}}^{\text{end}} P_d \, dt}{\int_{\text{start}}^{\text{mid}} P_s \, dt} = \frac{E_d}{E_s}, \tag{4}$$

where start, mid, and end represent respective splits in the simulation, P_d is power discharged, P_s is power stored, E_d is energy discharged, and E_s is energy stored. E_d ends up totaling 1.04×10^5 J (28.83 Wh) while E_s totals 1.21×10^5 J (33.67 Wh), resulting in an efficiency of 85.6%.

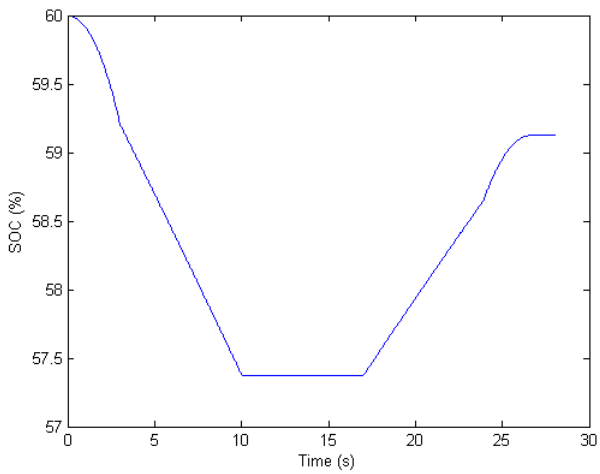

Figure 5: Battery State of Charge (SOC) vs. time

To corroborate this result, the efficiency at the battery (η_b) is calculated from its SOC using

$$\eta_b = \frac{\mathrm{SOC_{mid}} - \mathrm{SOC_{end}}}{\mathrm{SOC_{start}} - \mathrm{SOC_{mid}}} \tag{5}$$

As shown in Fig. 5, the SOC was initialized at 60% ($\mathrm{SOC_{start}}$), reduced during BEST storage to 57.38% ($\mathrm{SOC_{mid}}$), and finally increased during BEST discharge to 59.13% ($\mathrm{SOC_{end}}$). Eqn. (5) gives the round trip efficiency at the battery as 66.7%. When considering losses from the DC/DC converter and the internal resistance of the battery, this result corroborates well with the efficiency calculated in eqn. (4) especially considering general estimates of battery efficiency being in the 60-80% range [4].

This result is useful knowledge for the future development of a Parallel Hybrid Battery-BEST system. While BEST is shown in this simulation to have a response on the order of seconds, batteries can respond in milliseconds [4] making a combination of the two capable of grid frequency regulation as well as voltage regulation. Additionally, the power generated in the latter peak shown in Fig. 4 can be diverted to the battery for use in the following storage acceleration event, thus improving response times.

4 CONCLUSIONS

This paper has built upon previous work to present a refined dynamic model of BEST. Refinements included the use of a single IPMSM for both storage and discharge modes, the addition of damping forces to account for gearbox and rotating frictional losses, and a single simulation that demonstrates a complete cycle of operation. Based on power consumed by storage mode and power generated by discharge mode, the efficiency was calculated to be 85.6% at the PMSMD. Compared with other energy storage devices, this is competitive [4].

An additional goal was satisfied with this work, and that is that key components have been modeled after commercially available off the shelf (COTS) items which implies a relatively low cost prototype. The IPMSM is similar to that found in a hybrid electric vehicle drivetrain, as is the motor drive and the DC/DC converter. The gearbox has a common ratio, and wire ropes and reels can be sourced commercially as well as anchors.

5 FUTURE WORK

Near term future work includes the design of a feedback control methodology capable of consuming and producing variable power through torque regulated buoyant element speed manipulation. When connected to a utility scale power grid model, frequency changes can be used as an input, thus readying the model for simulations of high renewable energy penetration ratios and experimental mitigation of resource intermittency challenges.

Additional work includes the modeling of different BEST designs including a floating platform, pulley driven design. It is theorized that at larger scales, this layout will be more cost effective in terms of both capital and maintenance costs. The design, however, begs the additional modeling of disturbance forces caused by currents, tides, waves, and even tsunamis.

As working depths increase, modeling pressure and temperature effects on the buoyant element should also be undertaken to determine potential losses due to conductive heat transfer.

ACKNOWLEDGMENTS

This work is funded by the Renewable Energy for Island Sustainability (REIS) program at the University of Hawaii at Manoa and the Department of Energy's Workforce Training Initiative.

REFERENCES

[1] Ghorbani, R., Subsea Energy Storage and Recovery System, US. Provisional Patent Pending, Dec. 2009.

[2] Thornbrue, T., Ghorbani, R., *An Introduction to Modular Buoyant Energy Storage Technology.* Proc. MTS/IEEE OCEANS10 Conference in Seattle, Washington, 2010.

[3] Thornbrue, T., Ghorbani, R., *Development of Utility Scale Buoyant Energy Storage Technology.* Proc. OMAE2011 Conference in Rotterdam, The Netherlands, 2011.

[4] Alamri, B.R., Alamri, A.R., *Technical review of energy storage technologies when integrated with intermittent renewable energy*, Sustainable Power Generation and Supply, 2009. SUPERGEN '09 International Conference, pp.1-5, 6-7 April 2009.